Urban Climate 23 (2018) 287–308

Contents lists available at ScienceDirect

Urban Climate

journal homepage: http://www.elsevier.com/locate/uclim

Role of watering practices in large-scale urban planning strategies to face the heat-wave risk in future climate

M. Daniel [a,*], A. Lemonsu [a], V. Viguié [b]

[a] Météo-France/CNRS, Groupe d'étude de l'atmopshère météorologique, 42 avenue Gaspard Coriolis, 31057 Toulouse cedex, France
[b] Centre international de recherche sur l'environnement et le développement (CIRED), 45 bis avenue de la Belle Gabrielle, F-94736 Nogent sur Marne cedex, France

ARTICLE INFO

Article history:
Received 31 May 2016
Received in revised form 27 October 2016
Accepted 5 November 2016

Keywords:
Irrigation
Pavement watering
Urban heat island effect
Urban climate
Climate change
Adaptation

ABSTRACT

Increasing heat-wave risk due to regional climate evolutions, exacerbated by urban heat island (UHI) effects, is a major threat for the inhabitants of many cities. Adaptive policies such as greening the urban environment are often proposed to limit population vulnerability, as vegetation enables to regulate the microclimate by evapotranspiration. The efficiency of such strategies depends on water availability and raises the issues of water supply for irrigation and of vegetation efficiency. Three vegetation watering alternatives and a scenario of pavement watering are studied and compared using Paris (France) urban area as a case study. With an evolution of the city based on "business as usual" trends, urban climate modeling enables to evaluate both UHI and heat stress under heat-wave conditions in 2100. Vegetation watering is efficient in reducing air temperature and thermal stress, but mostly in residential areas where vegetation density is important enough. Pavement watering is relevant in the densely built city center only where it improves the cooling efficiency and increases the water consumption by 2% only. The combination of both solutions provides the best performances with a reduction (compared to a non irrigated scenario) of the maximum temperature anomaly by 0.8 °C (2.6 °C) during the day (night).

© 2016 Elsevier B.V. All rights reserved.

* Corresponding author.
E-mail addresses: maxime.daniel@meteo.fr (M. Daniel), aude.lemonsu@meteo.fr (A. Lemonsu), viguie@centre-cired.fr (V. Viguié)

http://dx.doi.org/10.1016/j.uclim.2016.11.001
2212-0955/© 2016 Elsevier B.V. All rights reserved.

1. Introduction

Climate change and global warming due to greenhouse gas emissions are already observed and are intensifying (IPCC, 2015). One of the consequences is an increase of summer heat-waves (IPCC, 2015, Giorgi, 2006). This has been highlighted by Déqué et al. (2007) for France at the national level by Lemonsu et al. (2014) for the Paris region, which could be affected by more than ten days of heat-wave per year on average by the end of the 21st century. This severe heat, exacerbated in cities by the urban heat island (UHI) effect (Basara et al., 2010; Tan et al., 2010; Gabriel and Endlicher, 2011; Li and Bou-Zeid, 2013), are already a clearly-identified public health concern, which is steadily growing (Lemonsu et al., 2013) and alarming institutional stakeholders (see for instance, Stone and Rodgers, 2001; Solecki et al., 2005; Hamin and Gurran, 2009; Lambert-Habib et al., 2013).

To face this issue, it is essential to devise, evaluate, and implement efficient climate change adaptation and UHI mitigation strategies. The countermeasures usually proposed to reduce air temperature in urban environment are either designed to modulate the thermo-radiative processes or the energy exchanges with the atmosphere. The first ones are related to a modification of the radiative properties of urban facets and building envelopes, e.g. with reflective materials (Santamouris and Kolokotsa, 2013; Kolokotsa et al., 2011), or the creation of shading areas by playing with urban form or trees (Potchter et al., 2006, Souch and Souch, 1993, Shashua-Bar and Hoffman, 2000). Some other techniques aim at modifying the surface energy balance by favoring water evaporation, in order to refresh the ambient air, while reducing heat convection and storage. This is possible with the use of pervious soils and vegetation, or through the wetting of urban surfaces.

Urban greening, i.e. adding vegetation in the city, is a solution more and more studied and promoted at different spatial scales (Gaffin et al., 2012; Rosenzweig et al., 2011; Bowler et al., 2010): green belts around the city (Masson et al., 2013b, Adachi et al., 2014), urban parks (Potchter et al., 2006), or green building envelopes (Wark and Wark, 2003; Alexandri and Jones, 2008; Jaffal et al., 2012; Malys et al., 2014). Pavement watering is a more recent approach that has been so far investigated essentially through experimental works (Takahashi et al., 2010; Hendel et al., 2015). Nonetheless, these various methods used to magnify evaporation are highly dependent on water availability. They may require an important water supply that must be quantified to objectively evaluate the strategy's viability. To the authors' knowledge, only few works raise this issue. Shashua-bar et al. (2011), especially, proposed an indicator of cooling efficiency, defined as the ratio between the daytime cooling and the equivalent latent heat from the evapotranspiration of plants. Based on measurements, different vegetation combinations have been evaluated (Shashua-Bar et al., 2011; Middel et al., 2012).

With the prospect of accelerating climate change, especially illustrated by an increase and intensification of heat waves, associated with the expansion of cities and their populations, the present paper aims at investigating the possible strategies for cities' evolution and adaptation at large scale. Special attention is paid here to the issue of city greening, and more importantly the associated watering practices, with the ambition of assessing the urban planning strategies on the basis of additional considerations that are rarely taken into account. However, the question of water resources and of their sustainable management, from the global scale to the level of municipalities and local authorities, is today a prevalent and essential issue.

2. Paris 2100 as a case study

2.1. Previous studies

The Paris urban area (France) is used here as a case study, considering that Paris conurbation is one of the most populated urban areas in the European Union with more than 12 million inhabitants in 2012 according to the INSEE French national statistics institute. It has been particularly affected by the European heat-wave of summer 2003 with about 5000 casualties (Hémon et al., 2003), and has been the subject of several studies about UHI mitigation strategies (see especially Masson et al., 2013b; Lemonsu et al., 2013, 2015; de Munck et al., 2013; de Munck, 2013; Kounkou-Arnaud et al., 2014).

The works of Masson et al. (2013b) have shown that urban planning at large scale has a major role to play on the UHI regulation. In this case, the planting of forests and vegetable crops around the city leads up to a 2 °C decrease of air temperature inside the city in case of heatwaves. More generally, the implementation of green or blue belts may influence local-scale meteorology and the flows around and above the city, and consequently refresh the city during summer periods. The modeling of the 2003 heat wave over Paris with the TEB urban

climate model coupled to the Meso-NH atmospheric model (Lafore et al., 1998) has enabled to assess various action levers at city scale, more especially the impact of greening and pavement watering (de Munck, 2013; Kounkou-Arnaud et al., 2014). De Munck (2013) has investigated the cooling potential of green roofs and ground-based vegetation, on the basis of realistic scenarios for which vegetation is implemented in the existing city only where possible. They have showed that vegetation water supply is essential in order to obtain a cooling effect. In addition, Kounkou-Arnaud et al. (2014) have tested the innovative solutions of pavement watering using a similar numerical setup. They obtained a slight decrease in air temperature in the streets of about 0.5 °C in the afternoon, significantly smaller than the 2 °C cooling obtained with watered ground-based vegetation.

2.2. The VURCA project

This study is in the line of the previous works but aims at adopting a more prospective and integrative approach by accounting for evolution of the city itself and modification of climate. This was the objective of the VURCA national research project which ambitioned to assess the vulnerability of Paris to future heat waves and to propose adaptation strategies. By using an interdisciplinary and systemic modeling system for the city, we had been able to provide quantitative estimates of the potential benefits of various strategies for evolution of city and of some practices. The efficiency of strategies has been assessed through diagnostics or indicators that cover different thematic areas: urban climate, thermal comfort, energy consumption of buildings, and water consumption. Starting from the multiple scenarios studied, a first study has been conducted on the impact of urban expansion scenarios on urban heat island and heat stress in Paris (Lemonsu et al., 2015). The results have highlighted that the exposure of inhabitants to heat is lower in case of a city less compact and greener.

However, the starting assumption was that urban parks and gardens were systematically watered, which is not necessarily realistic under heat wave condition. A more specific analysis is conducted here in order to compare various strategies of water use either for vegetation irrigation or pavement watering. The objective is to evaluate their efficiency by putting in perspective the gains in terms of UHI mitigation and thermal comfort improvement, and the induced water consumption. In addition, one can expect that this efficiency varies depending on intensity and duration of heat waves.

After a description of the global methodology in Section 3, this paper investigates the impacts of different scenarios of vegetation irrigation or pavement watering on evaporation (Section 4) and UHI patterns (Section 5). Section 6 examines the efficiency of each scenario in terms of temperature and thermal comfort, and finally Section 7 discusses the variabilities and uncertainties of our results, and Section 8 concludes.

3. Methodology

3.1. General modeling methodology

The study presented here uses the methodology developed within the framework of the VURCA research project, described in detail in Lemonsu et al. (2015). The urban climate of Paris is simulated using a physically-based urban canopy model. Due to recent developments, this model is sophisticated enough to simulate, at the city scale, air temperatures inside and outside the buildings, indexes of thermal comfort, air-conditioning systems (energy consumption, associated heat release and potential feedback on air temperature outside), as well as evapotranspiration of plants in urban environment.

Instead studying a past heat wave to illustrate what could be the future events (Beniston, 2004; Vautard et al., 2007), a set of synthetic or theoretical future heat waves has been built. These events vary in intensity (daily maximum temperature) and in duration (number of days) with variation ranges defined from the analysis of regional climate model projections (Lemonsu et al., 2014).

By addressing the climate change issue in cities, and by working on long timeframes up to the end of the 21st century, it is important to also take into account the evolution of city characteristics. These different processes that interact locally can significantly modify the urban temperatures, energy demand, or water consumption, compared to present situation. Consequently, among the ensemble of city scenarios built in the VURCA project, we use here a reference prospective scenario which assumes evolutions for city characteristics that follow current trends (detailed hereafter).

3.1.1. Heat-wave and urban climate modeling

The urban climate of Paris is simulated using the physically-based urban canopy model, Town Energy Balance (TEB), (Masson, 2000; Hamdi and Masson, 2008). This model simulates at the same time, meteorological conditions, at street-level and inside buildings, through a specific coupled building energy model (Bueno et al., 2012; Pigeon et al., 2014). Moreover, using near-surface air temperature, humidity, wind speed, as well as incoming solar and infrared radiation, the model also computes the Universal Thermal Climate Index (UTCI), (Fiala et al., 2012). This is a modeling of the estimated thermal comfort of the human body (see COST Action 730, http://www.utci.org). This index is computed by TEB model, both inside the buildings and in the streets, at each grid cell of the modeling domain.

In order to better represent urban green areas and catch the interactions between build-up and natural covers (Lemonsu et al., 2012), TEB is coupled with the Interaction Soil Biosphere Atmosphere (ISBA) model (Noilhan and Planton, 1989). ISBA is a Soil Vegetation Atmosphere Transfer model that computes the surface radiative (direct and diffuse solar radiation and infrared radiation) and energy (latent, sensible and storage heat fluxes) budgets for natural soils and vegetation. It also simulates water exchanges that include plants transpiration, evaporation of water intercepted by the foliage, evaporation from the ground, as well as several hydrological processes (drainage, infiltration and capillary attraction in the soil). By accounting for these water exchanges and the hydrological properties of the ground, and based on a three-layer vertical discretization of the soil column, the model computes the evolution with time of the soil water contents (Boone et al., 1999). ISBA is also able to simulate different types of vegetation, especially by varying the vegetation fraction, the leaf area index, or the stomatal resistance. These processes are included in the urban climate modeling, so that the resulting model is able to quantify their cooling effects on the city. It is however important to emphasize that the current version of TEB-ISBA does not consider in the radiative budget the shadow effects of trees on walls and ground-based surfaces (Lemonsu et al., 2012).

On the basis of 1-km spatial resolution atmospheric simulations of the 2003 heat wave performed by de Munck et al. (2013) and Kounkou-Arnaud et al. (2014) for Paris region, we have built a set of synthetic heat waves of variable intensities by modulating the real meteorological conditions (maximum daily temperature, humidity, and incoming longwave radiation). The duration of the event can also be adjusted by replicating the daily meteorological conditions day after day. Four different intensities are considered, corresponding to a daily maximum temperature of 34, 38, 42, and 46 °C (referred to as HW34, HW38, HW42, and HW46, respectively). These intensities have been defined according to a statistical analysis of future heat waves over Paris basin simulated by an ensemble of regional climate models (Lemonsu et al., 2014). Note that the synthetic heat wave HW38 for a duration of seven days is quite comparable to the real 2003 heat wave. These meteorological forcings are used to run the TEB-ISBA surface model in an offline mode, to assess the sensitivity of the urban climate to irrigation practices for variable heat-wave conditions. In this paper, we will mostly focus on the seven-day HW38. However, a sensitivity to heat-waves intensities and durations is carried out in Section 7.

Initial conditions, especially the soil water content to which results can be quite sensitive, are defined the same way for each irrigation scenarios, starting from the complete simulation of the 2003 heat wave performed by de Munck et al. (2013). Note that the simulation of de Munck et al. (2013), conducted with the Meso-NH non-hydrostatic model (Lafore et al., 1998) coupled to the TEB model, had been evaluated using local observations in Paris region. In addition, the methodology of urban climate modeling adopted in VURCA project, for which the TEB urban canopy model is initialized using a city description provided by the urban expansion socio-economic model (see next Section), has been also evaluated for one day of the 2003 heat wave. Detailed results are available in Lemonsu et al. (2015).

3.1.2. Urban expansion modeling and city evolution

TEB-ISBA model is run over a domain of 100 km × 100 km centered on Paris city center with a horizontal resolution of 1 km (see the domain in Fig. 1). To fulfill the requirement of the VURCA project, an urban expansion scenario of Paris urban area is simulated until 2100 using the NEDUM-2D model (Viguié et al., 2014). This socio-economic model simulates the spatial distribution of land and real estate values as well as the main characteristics of the city such as population and building density, green and housing areas. It is based on a dynamic extension of the urban economic theory (Fujita, 1989). Simulated city shape evolution and characteristics have been calibrated over the period 1900–2010, and details of its calibration are presented in Viguié et al. (2014).

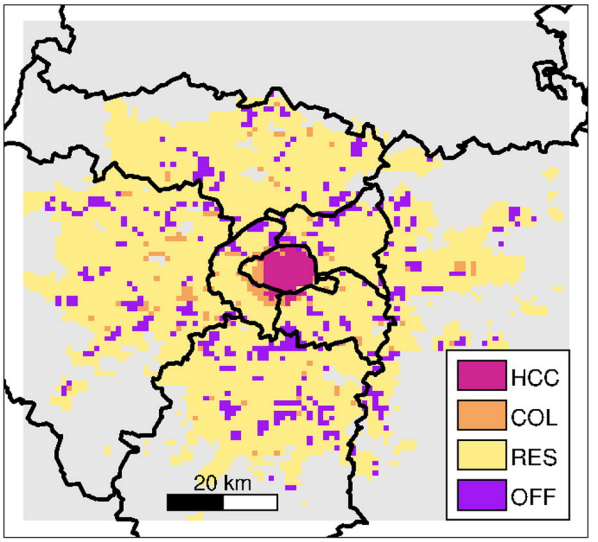

Fig. 1. Spatial extent of the Paris conurbation simulated in 2100 by the NEDUM model. Urban areas are classified in four typologies: historical city center (HCC), collective housing (COL) and residential housing (RES), and office buildings (OFF).

Beyond 2010, the urban expansion dynamics follows a scenario based on current trends of population density decrease, and on a moderate total population increase scenario (+9% in 2100) (see Appendix A): we suppose that no specific urban policy or regulation is implemented in order to limit urban sprawl, so that the city still grows following the current trends. The simulated city in 2100 covers 3090 km^2 including 1420 km^2 of green areas (gardens and public parks) for a demographic projection of 13,400,000 inhabitants.

The buildings are classified in four architectural typologies (see map in Fig. 1) historical buildings located in the city center (Haussmannian architecture buildings dating from 19th century and referred to as HCC), collective housing (COL), single housing (RES), and office buildings (OFF). Materials characteristics of buildings and renovation techniques are specified differently for each typology on the basis of an inventory of the current Parisian buildings and the renovation trends.

Projected buildings characteristics in 2100 are based on the assumption that the energetic performances of buildings are going to improve with time due to the technological progresses in construction and renovation methods, following current trends. A complete database of buildings characteristics, built for the VURCA project (Marchadier et al., 2012), is used here. It is assumed that all collective housing (COL) and single housing (RES) buildings follow the French thermal regulations of 2012. The level of renovation is higher for office buildings which are equipped with high-performance vacuum insulation systems and reflective materials. Inversely, because of architectural and aesthetical reasons, the historical buildings (HCC) are the least renovated ones (a simple interior thermal insulation is implemented in this case).

3.2. Evaporation processes and water use for refreshing

3.2.1. Vegetation watering

Evapotranspiration-related thermal-regulation capacity of vegetation in urban environment is tightly related to water availability. Two mechanisms are involved with different dynamics. First, soil water, as well as the water intercepted by the foliage after a period of rainfall or watering, can evaporate. This physical process can take place either day or night. The response to a punctual water supply is quick for water intercepted by the foliage and slower for soil water. This phenomenon is affected by environmental conditions, especially atmospheric water pressure. Water exchanges are also induced by plants transpiration. This physiological mechanism, coupled to photosynthesis, takes place during the day (for most of vegetal species) and is based on water extraction from the soil by the roots and water evaporation by the leaves through the stomata.

The ISBA model - which is part of Surface Vegetation Atmosphere Tansfer (SVAT) type models - simulates the physiological processes that manage evapotranspiration of vegetation. It also includes a physically-based modeling of hydrological processes, so that it simulates the soil water status evolution and the retroaction on transpiration capacity of plants. The modeling of these processes in ISBA is detailed in Appendix B.1. Using this model, the vegetation watering practices can be represented. It can deal with different forms of water inputs either on vegetation, at the ground, or in the soil, and the way this water is used by the soil-plant system.

3.2.2. Pavement watering

In densely-built urban environment, pavement watering can be a solution to mitigate UHI. The water sprinkled on the pavement is rapidly evaporated during hot conditions, which cools the ambient air while limiting surface warming. This refreshing strategy offers the advantage of responding quickly to a punctual watering. The evaporation potential is however strongly constrained by the maximum capacity of water storage on roads. Beyond a certain water quantity, the surplus is lost by surface runoff toward sewers.

Based on experimental works, Takahashi et al. (2010) studied and quantified the impact of this practice on local air temperature. They found that in case of high air temperatures greater than 30 °C in the city, air temperature can decrease by about 2 °C in the morning and 4 °C in the afternoon. Various experimental protocols were tested and the most important cooling effects were measured when sprinkling for three minutes every 30 min with a rate of 0.33 L m^{-2} min^{-1}. Another experimental sensibility analysis was performed during summer 2013 by Hendel et al. (2015). It was found that for sunny days pavement watering should be activated every 30 min with a rate of 0.31 to 0.41 L m^{-2} h^{-1}. Using this set-up, he found that surface temperature could be reduced by 4 °C in the morning and up to 13 °C in the afternoon. He also found a gain of 2.3 °C to 5.9 °C of temperature 5 cm below the surface, proving that pavement watering is efficient when aiming at decreasing heat storage in impervious surfaces.

The TEB models are one of the few urban climate models that include surface water exchanges. The current parameterization is rather simple, but enables to represent rainwater interception on roads and roofs, evaporation of available water, and surface runoff (see Appendix B.2 for details). The implementation of pavement watering in TEB is based on this parameterization, simply by treating this water supply the same way than rainfall on roads.

3.2.3. Irrigation scenarios

The configuration used here as reference scenario is the simulation performed without anthropic water supply for vegetation during the whole heatwave (simulation referred to as *REF*). It is assumed that no water is available for other actions than daily life usages, so that private gardens and urban parks are not watered.

Two alternatives for vegetation (public parks and private gardens) watering, which represent 1419 km^2 (see Table 1), are then tested and simulated, in order to assess their impacts on soil water status, surface energy balance, local microclimate, and comfort conditions. Watering aims at maintaining sufficient soil

Table 1
Assessment of water consumptions the different irrigation scenarios: Unrestricted (R), Pavement watering (P), Realistic (R) and Combined (C). These consumptions are compared with water consumption in 2009, the mean and low flows of the Seine River and the expected Seine mean flow in 2100.

		(U)	(P)	(R)	(C)
Watered surfaces (km^2)	Gardens/parks	1419	0	1419	1419
	Pavements	0	603	0	24
Water demand ($10^6 m^3.day^{-1}$)		5.5	1.5	4.9	5.0
% 2009 water consumption (2.37 $10^6 m^3.day^{-1}$)		232.1	63.3	209.7	211.0
% Seine mean flow (328 $m^3.s^{-1}$)		18.7	5.1	17.3	17.5
% Seine low flow (66 $m^3.s^{-1}$)		93.0	25.4	86.0	87.1
% 2100 Seine mean flow (230 $m^3.s^{-1}$)		26.7	7.3	24.6	25.0

moisture for plants but it is difficult to compute the quantity of water needed, as the transpiration intensity and the water quantity exchanged with atmosphere are controlled by the environmental conditions (sunlight, temperature, wind…), the soil water status, and the plant intrinsic properties such as stomatal conductance and leaf area index.

The first one is a realistic irrigation alternative (referred to as *R*), based on the most common watering practices in Paris according to de Munck (2013). An irrigation by sprinkling is activated at night from 11 pm to 7 am with a water supply of 1.2 10^{-7} m^3 s^{-1} (i.e. about 3.46 L per day and per m^2 of garden). Notes that it is generally recommended to water plants at night because, during the day, water loss by evaporation significantly reduces the water supply for the soil, and the water droplets on the leaves magnify the sunlight and threaten to burn the foliage (see de Munck, 2013). From a technical point of view, this irrigation process is modeled in TEB-ISBA as an input water flux that is received by soil and vegetation (as it is already done for rainfall, for instance). By modeling water supply this way, a part of water (depending on leaf area index of vegetation) is intercepted by the foliage, and consequently can be directly evaporated (see Appendix B.1).

The second scenario (referred to as *U*) represents an "unrestricted" water supply for urban vegetation. It is a maximalist scenario. In this case, the soil water content w_g of the ISBA model is controlled and adjusted at each time step of the simulation, so that the soil water reservoir is always at least half-filled. This is done by verifying that the soil wetness index (SWI) is always equal or greater to 0.5. This index is computed as follows:

$$\mathrm{SWI} = \frac{w_g - w_{wilt}}{w_{fc} - w_{wilt}} \geq 0.5 \tag{1}$$

with w_g the soil water content computed at each time step, and w_{wilt} and w_{fc}, the water contents at the wilting point and the field capacity, respectively. This approach is not realistic in a physical sense but aims at insuring a maximal evapotranspiration of plants and at assessing the associated cooling potential. Note that in this configuration, water is directly injected in the ground so that there is no surface evaporation as in the previous case. The issue is that for this simulation, no diagnostic in the model allowed us to compute the water needed to fill the soil layer. We assumed then afterwards that the water supply is at least equal to the evapotranspiration that occurred.

In addition, a scenario of pavement watering (referred to as *P*) is simulated in the present study. Watering is set-up for sidewalks alone (603 km^2, see Table 1), assuming they covers 50% of the pavement surfaces (1206 km^2, see Table 1). The water supply is based on a sensitivity study conducted within the frameworks of the EPICEA project (Kounkou-Arnaud et al., 2014). We suppose that the pavements is watered at a rate of 1.1 10^{-6} m^3 s^{-1} during three minutes at the beginning of every hour between 8 am and 8 pm (i.e. about 2.77 L day^{-1} and per m^2 of roads). For higher sprinkling rates, the water quantity is greater than the maximum storage capacity of the road reservoir simulated in the model (Masson, 2000, Lemonsu et al., 2007), so the water excess would be lost by surface runoff to the sewer (see Appendix B.2). Note that in this scenario, gardens and parks are not irrigated at all in order to be able to assess separately the different practices.

4. Impacts of watering on evaporation

For clarity and simplicity, the analysis of processes is firstly carried out and discussed within the framework of the heat wave HW38 with a duration of seven days, quite comparable to the real 2003 heat wave as indicated previously.

4.1. Reference case

Fig. 2 (top) shows, for scenario (*REF*) and for day seven, the daily cycle of latent heat flux (Q_E) in W m^{-2} in both historical city center (HCC) and residential areas (RES) (cf. the map in Fig. 1). Without any water supply on impervious surfaces, this flux includes only contributions from natural covers through soil evaporation and vegetation transpiration.

In RES, Q_E reaches a maximum of 73 W m^{-2} at midday after seven days of heat wave, whereas it is negligible at night when vegetation is photosynthetically inactive. The absence of irrigation results then in an important water stress for vegetation which significantly limits the relevance of greening strategies. In HCC, Q_E does not exceed 11 W m^{-2} in the middle of the day due to the predominance of impervious covers in this area.

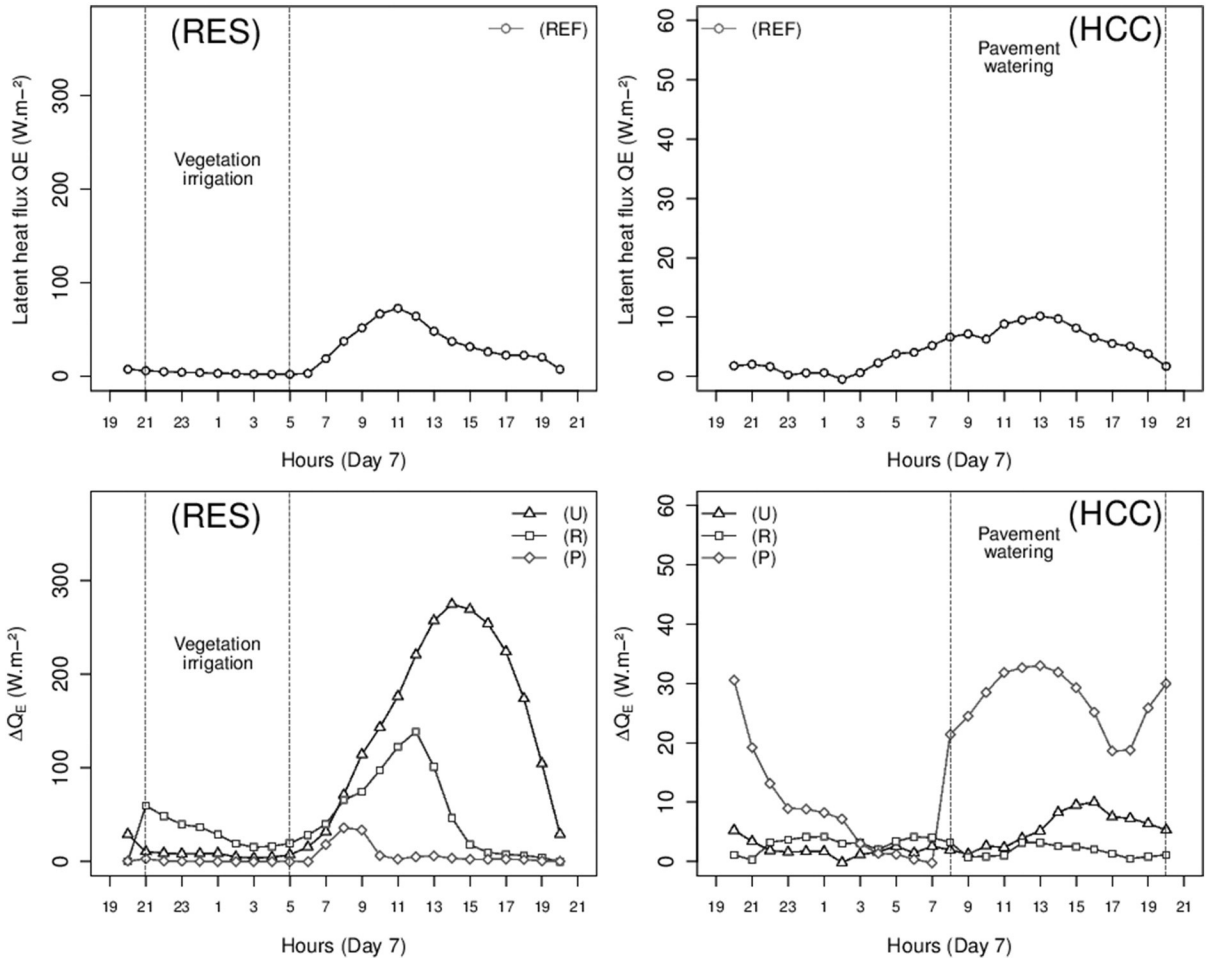

Fig. 2. Top: daily cycle of latent heat flux for the reference case. Bottom: difference between daily cycles of latent heat flux of each watering scenario and reference case. In both cases, fluxes are spatially aggregated over RES area (left) and HCC area (right). The dashed lines delimit the time periods of vegetation and pavement watering.

4.2. Benefits of watering strategies

Fig. 2 (bottom) shows the difference in latent heat flux between every scenario and the reference (*REF*).

In RES (Fig. 2), the vegetation watering boosts transpiration of plants so that Q_E increases by $+274$ W m^{-2} and $+138$ W m^{-2} for (*U*) and (*R*), respectively. One notes that during the day, (*U*) maintains the evaporation cycle until 2100 UTC, whereas it stops much earlier in (*R*). This highlights then the need for the vegetation to be irrigated in order to conserve its transpiration potential. Inversely, the evaporation of water intercepted by leaves during watering (see Appendix B.1) induces an additional evaporation phase in (*R*) overnight, with fluxes up to 60 W m^{-2}. (*P*) does not seem to provide any improvements except for the three first hours of watering with additional fluxes up to 50 W m^{-2}. Looking at the differences between the scenarios, one can conclude that irrigation is mandatory to keep a significant vegetation evaporation.

In HCC, the additional evapotranspiration is limited in the two scenarios based on vegetation watering (*U*) and (*R*) since the vegetation cover fraction is low. For (*U*), Q_E is however doubled in the afternoon ($+10$ W m^{-2}) compared to the reference. The pavement watering (*P*) is here more efficient. It leads to an additional Q_E up to $+33$ W m^{-2}. In this part of the city, the roads provide an important surface area for sprinkling, and consequently offer a higher evaporation potential than vegetation.

5. Impacts of watering on urban heat island

5.1. Reference case

For the reference scenario, the daily maximum daily temperature after seven days of heat wave is about 40 °C all over the urban area. At night, the minimum daily temperature varies between 25.8 °C in residential areas and 28.4 °C in the city center. By way of comparison, one can remind that the temperature thresholds that are prescribed for heat wave warning over Paris region are 18 °C and 34 °C for minimum and maximum daily temperatures, respectively (Lemonsu et al., 2014). This highlights the extreme conditions of this heat wave which is comparable to the 2003 heat wave. Maps of UHI are calculated as the difference between the local air temperature (temperature simulated by TEB-ISBA model 2 m above the ground) and a reference temperature corresponding to the temperature of rural areas, i.e. the mean temperature of peripheral and uninhabited grid cells. More details on the method can be found in Lemonsu et al. (2015). Maps of daytime and nighttime UHI are produced by averaging the model outputs between 1400 and 1600 UTC, and between 0200 and 0400 UTC, respectively.

During the day (Fig. 3, left), the UHI is large (3040 km^2 are impacted by an UHI greater than 1.5 °C, i.e. about 98% of the city area) with peaks of intensity that occur in the suburbs. Indeed, shading effect of buildings in the city center reduces the intake of solar radiation. That gives a maximal UHI in the city center of 1.3 °C compared to 2.5 °C in the suburbs. As already mentioned by Lemonsu et al. (2015), at night (Fig. 3, right) the UHI has a different pattern: it is less extended than during the day but reaches higher values in the

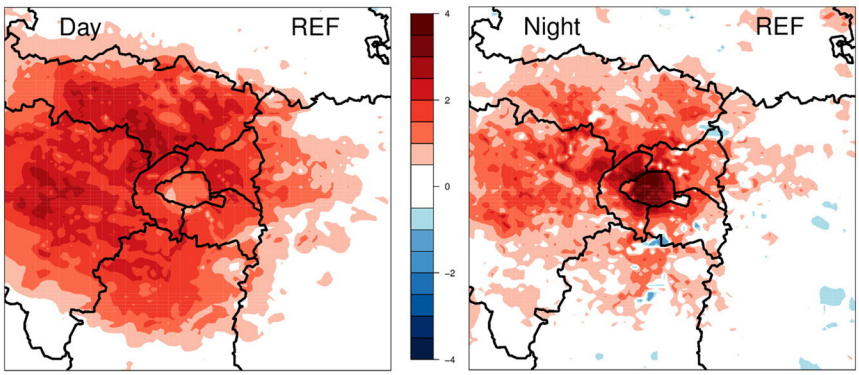

Fig. 3. Spatial representation of UHI for the HW38 after seven days of heat wave both for daytime (left) and nighttime (right) hours.

most urbanized areas. The maximum UHI intensity of 3.2 °C is to be found in the city center and the area covers by an UHI greater than 1.5 °C diminishes to 817 km^2, i.e. 26% of the city area.

5.2. Benefits of watering strategies

The benefits of watering strategies on UHI are computed as the difference between the reference scenario (*REF*) and every others scenarios. The maps of UHI mitigation are presented in Fig. 4 for daytime hours and in Fig. 5 for nighttime hours.

During the day (Fig. 4, left), in the unrestricted irrigation scenario (*U*), the city is almost unaffected by a 1.5 °C UHI (only 2% of the urban area is affected) thanks to an abundant evapotranspiration of green areas that efficiently decreases air temperature. The cooling, when compared to the reference scenario, reaches 1.0 °C in the city center and up to 3.8 °C in suburban areas. It hence confirms the importance of watering vegetation to maintain a potential cooling effect. The pavement watering (*P*) and realistic irrigation (*R*) scenarios lead to in-between results. Each of them has a distinctive pattern. Pavement watering alternative induces a cooling that goes up to 1.0 °C but that is located in the city center only. This is due to the fact that the fraction of the ground occupied by roads is small in suburban residential district (roads represent 31% of ground surfaces in residential areas). Results are almost opposite in the realistic irrigation scenario, with a mitigation of the UHI in suburban areas of 0.8 °C and a limited impact in the center. This is due to the fact that the proportion of green spaces is low in the city center and high in suburban residential districts. Therefore, the significant evapotranspiration cooling that occurs in residential neighborhood is not allowed in densely built areas.

At night (Fig. 5, right), the pavement watering has a limited impact since it is activated only between 8 am and 8 pm and water evaporates rapidly on impervious surfaces. A slight but not significant cooling (less than 0.5 °C) is however noted in the city center compared to (*REF*) because during the day the roads consume a large part of the energy they received by evaporation and they consequently store less heat. For both scenarios (*U*) and (*R*), a UHI mitigation between 0.5 and 1.5 °C is displayed in residential areas, and the realistic irrigation scenario appears even more efficient than the unrestricted one. Actually, at that time of the day, both types of irrigation are activated but do not apply in the same way. For unrestricted irrigation, water is directly injected in the ground (see Section 3.2.3) and taken by the roots for transpiration of plants mainly during the day. For realistic irrigation, the vegetation is watered by sprinkling, so that a part of the water is intercepted by the foliage and can be directly evaporated, thereby inducing a nocturnal cooling. Therefore the cooling (up to 2.2 °C) observed for (*U*) is due to a lower daily heat storage while for (*R*) cooling up to 2.6 °C is explained by the lower daily heat storage but also by the significant evaporation at night (see Section 4.2).

5.3. Combination of watering practices

The watering of vegetation and pavement are two solutions that enable a local cooling effect, each by operating on a specific environment (natural or impervious covers) through different physical processes. They can consequently be combined to maximize the UHI mitigation, by adapting their implementation according to the areas where they are the most efficient.

The combined scenario (referred to as *C*), which combines irrigation of urban green areas (according to the same protocol than for the realistic irrigation scenario (*R*), see Section 3.2.3) and pavement watering only for roads of the city center and inner suburbs, leads to the maximal cooling both at daytime and nighttime, whether in residential areas and city center.

As can be seen on Fig. 6, such a combined scenario cumulates the benefits of the two options. During the day and at night, the temperature decreases both in the city center (with a maximum decrease during the day of 1.1 °C) and in suburban areas (with a maximum decrease at night of 2.6 °C). At night, the maximum temperature anomaly is noticeably lowered with a gain of 0.6 °C, 0.3 °C and 0.4 °C compare to (*REF*), (*R*) and (*P*), respectively. At that time of the day, the area of the city affected by a 1.5 °C UHI (164 km^2) is 79% smaller than for (*REF*) but is however not significantly smaller than for (*R*) (173 km^2). During the day, the maximum temperature anomaly is reduced by 0.8 °C compare to (*REF*). The comparison of (*C*) with (*R*) (respectively (*P*)) leads to a reduction of UHI spatial extent of 8%, i.e. 79 km^2 (respectively 56%, i.e. 1130 km^2) while the maximum temperature anomaly is reduced by 0.4 °C (0.2 °C).

However, these results must be tempered. In terms of real air temperature, the combined scenario leads to minimum daily temperatures of 24.93 °C on average, and maximum daily temperatures of 39.48 °C. Despite a

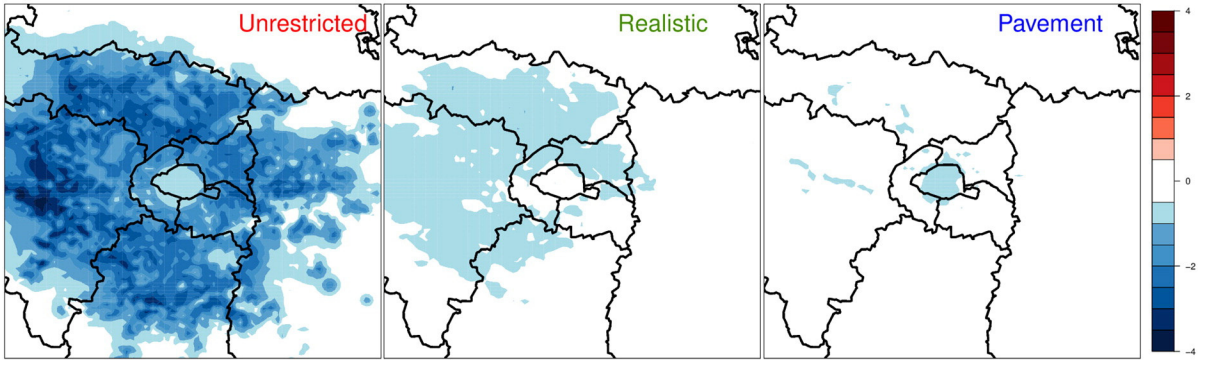

Fig. 4. Maps of 2-m air temperature difference between each watering scenario and the reference for daytime hours. Results are presented here for the HW38 after seven days of heat wave.

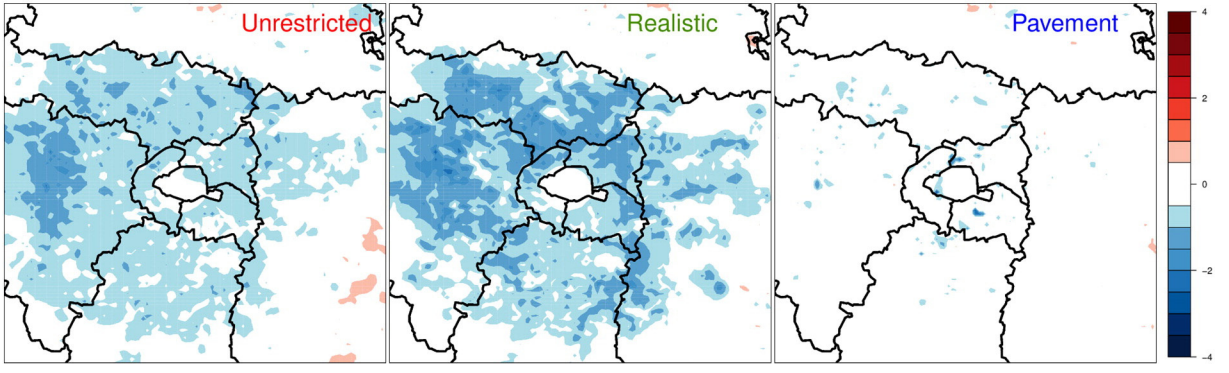

Fig. 5. Maps of 2-m air temperature difference between each watering scenario and the reference for nighttime hours. Results are presented here for the HW38 after seven days of heat wave.

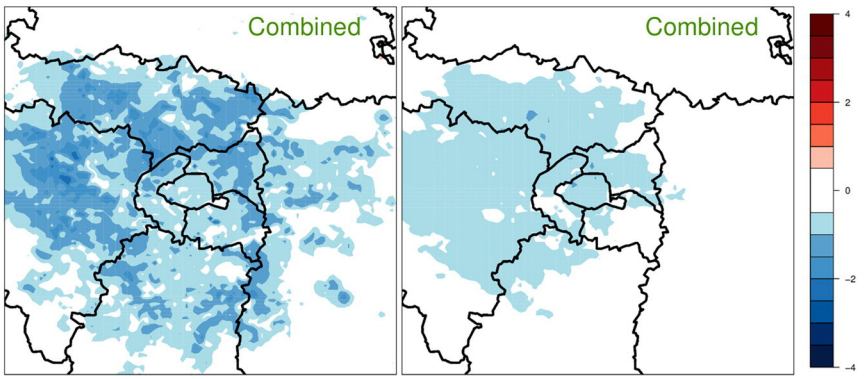

Fig. 6. Maps of 2-m air temperature difference between combined scenario and the reference for daytime (left) and nighttime (right) hours. Results are presented here for the HW38 after seven days of heat wave.

significant mitigation effect in comparison to the reference situation, these temperatures remain very high and correspond to high discomfort conditions. More especially in the city center at night, the air temperatures do not decrease so much (27.81 °C in the city center against 24.94 °C in the residential areas). This illustrates the population exposure to the warm nocturnal conditions that can occur during heat waves and lead to public health issues (Laaidi et al., 2012).

6. Efficiency of watering strategies

The gain of temperature due to vegetation irrigation or pavement watering must be put in regard with the water demand associated to each strategy. For each scenario a cumulative cooling effect (in K day^{-1}) is calculated as the sum of hourly differences in 2-m air temperature (T_{2m}) between a given scenario (SCE) and the reference case (*REF*).

This cumulative cooling effect is computed for all the duration of heat wave, and then expressed on one average day.

$$\Delta \mathrm{T2m}^{\mathrm{SCE}}(d,i) = \frac{\sum_{h=1}^{h=24*d} \left(\mathrm{T2m}^{\mathrm{SCE}}(h,i) - \mathrm{T2m}^{\mathrm{REF}}(h,i)\right)}{d} \tag{2}$$

The spatial field of daily cooling that is obtained in this way is finally aggregated by summing all grid-point values and by weighting them according to the urbanization rate at each grid-point. The urbanization rate is the fraction of urban covers in each grid-point that includes buildings, ground-based impervious covers, and

Table 2
Cooling efficiency coefficients (spatially averaged temperature decrease, in °C, per total Mm^3 of water) of watering scenarios evaluated for HW38 after seven days of heat wave. The coefficients are calculated based on map of urbanization rate or of population density, and starting from the 2-m air temperature (Eff) or the UTCI (Eff').

	(P)	(R)	(C)
Eff (plain spatial average)	5.496	4.656	4.824
Eff (average taking into account population density)	7.512	4.008	4.920
Eff' (plain spatial average)	8.856	4.560	4.872
Eff' (average taking into account population density)	12.624	3.768	5.520

urban vegetation:

$$\Delta T2m^{SCE}(d) = \frac{\sum_i \left(\Delta T2m^{SCE}(d,i) \cdot f_{town}(i)\right)}{\sum_i f_{town}(i)} \quad (3)$$

Finally a dimensional cooling efficiency coefficient (Eff in K per Mm^3 of water) defined as the ratio between this cooling effect , and the daily water consumption for the considered watering scenario (V_{wat} in Mm^3 day^{-1}) is computed:

$$Eff_{(R)} = \frac{\Delta T2m^{SCE}(d)}{V_{wat(R)}} \quad (4)$$

For this calculation (here is the example of (R) scenario), the differences in T_{2m} calculated at each grid point of the modeling domain are spatially aggregated at city scale either according to the map of urbanization rate, or according to the map of population density (provided by the NEDUM simulation).

Another way to compute the cooling efficiency coefficient (Eff') is to consider the UTCI difference computed between the watering scenario and the reference (also expressed in K day^{-1}) instead in 2-m air temperature:

$$Eff'_{(R)} = \frac{\Delta UTCI^{SCE}(d)}{V_{wat(R)}} \quad (5)$$

6.1. Water consumption

The average daily water demand is calculated for each scenario and presented in Table 1. Obviously, in the absence of irrigation (*REF*), no water is needed. For (*U*), the daily water supply is calculated from the difference in evapotranspiration fluxes between the scenarios (U) and (*REF*), by assuming that the additional water quantity that is exchanged with atmosphere by evapotranspiration for the scenario (*U*) in comparison with (*REF*) is directly comparable to the water quantity injected in the ground. For (*R*) and (*P*), daily water supplies are constant and then directly calculated according to the prescribed watering rates (see Section 3.2.3).

The higher water consumer scenario is (*U*) which requires 5.48 10^6 m^3 of water per day (see Table 1). In comparison, the realistic irrigation (*R*) consumes only 10% less (4.90 10^6 m^3 day^{-1}) whereas the pavement watering (*P*) only requires 1.55 10^6 m^3 day^{-1}, i.e. 72% less. The combined scenario (*C*) requires 4.97 10^6 m^3 of water per day, i.e. less than 2% more than vegetation irrigation (*R*) scenario alone. Note that by activating pavement watering only in the central area of the city, the water consumption for this use is reduced by more than a factor of ten compared to the scenario (*P*).

A reference can be made to the current water consumption of the city of Paris, i.e. 0.55 10^6 m^3 day^{-1}. Since this quantity is only available for inner Paris it cannot be compared to vegetation irrigation strategy. But it can be put in perspective with the water consumption for pavement watering in Paris city center which is equal to 0.067 Mm^3 day^{-1} (corresponding to the difference in water consumption between (*C*) and (*R*)). During heat wave conditions, the pavement watering would lead to an increase of 12% of the current water consumption of the city of Paris. In addition, the water consumption of all scenarios can be compared to the amount of water withdrawn for consumption which was about 2.37 10^6 m^3 day^{-1} (http://www.statistiques.developpement-durable.gouv.fr). As expected, the city area being much larger in 2100, the combined scenario would then lead to an important increase of 110% of the water demand (see Table 1). There consumptions can also be put in regard with the mean flow of the Seine River which is currently about 28.3 10^6 m^3 of water per day and could be reduced by 30% in 2100 due to climate change and increase in droughts (Ducharne et al., 2009). This reduction would have an indirect impact on the available water for irrigation and evapotranspiration by modifying underground water and soil water content.

Table 1 indicates the proportion of water demand compared with the 2009 consumption, the current mean flow and low flow of the Seine River, and the mean flow of the Seine River projected in 2100 according

to the results of the RExHySS project (Ducharne et al., 2009). Thus, for the combined watering scenario, water consumption represents 17% of the current mean flow of the Seine River and up to 87% under low flow condition. In 2100, it could be equivalent to a quarter of the mean flow of the Seine River and probably exceed the low flow. This emphasizes the need for an optimization of watering practices and a more sustainable and sensible use of water resources.

6.2. Cooling efficiency

The cooling efficiencies of watering scenarios (*P*), (*R*), and (*C*) in relation to the reference case (*REF*) are evaluated and compared. As explained before, the cooling efficiency coefficient (Eff) is spatially averaged according to the maps of urbanization rate or of population distribution. The results are presented in Table 2 and Fig. 7.

The most efficient scenario is the pavement watering (*P*) whatever the method of calculation for cooling efficiency coefficient. In this case, $Eff_{(P)}$ reaches about 5.5 and 7.5 K per Mm^3 of water based on urbanization and population distribution, respectively, whereas $Eff_{(C)}$ and $Eff_{(R)}$ range from 4.0 to 4.9 K per Mm^3. However, even though it is more efficient because it consumes little water, (*P*) does not allow high cooling values: ΔT_{2m} is limited to -8.5 K day^{-1} in this case while it goes up to -22.8 K day^{-1} and -24.0 K day^{-1} for (*R*) and (*C*), respectively.

It is interesting to emphasize that $Eff_{(P)}$ is still better when it is calculated on the basis of population distribution (7.5 instead 5.5 K per Mm^3) because the pavement watering is especially efficient in the most populated areas in the city center and inner suburbs. Inversely, $Eff_{(R)}$ is weaker when calculated this way (4.0 instead 4.6 K per Mm^3). The combined scenario which cumulates the benefits of both watering strategies presents equivalent efficiencies $Eff_{(C)}$ of 4.8–4.9 K per Mm^3.

Finally, when the cooling efficiency coefficients are computed using the UTCI rather than the 2-m air temperature, the results are significantly different, more especially for pavement watering (see Table 2). As a reminder, the UTCI is a measure of individual thermal comfort which takes into account not only air temperature but also humidity, wind speed and radiation. By watering the pavement, one considerably limits the daytime warming of ground-based impervious surfaces (especially the road), so that their infrared emissions are strongly reduced, which limits the UTCI increase. Indeed, UTCI is then reduced thanks to a lower air temperature but also and mostly thanks to a diminution of the radiation emitted by the road. Very high coefficients of cooling efficiency are consequently obtained: $Eff'_{(P)}$ is 8.5 and 12.6 K per Mm^3, based on urbanization and population distribution, respectively.

7. Variability and uncertainties of impacts

The results obtained and discussed in this study are strongly dependant on the hypotheses chosen for the simulations. Let us examine in this section how a change in these hypotheses might affect our results.

7.1. Urban expansion

In all the simulations of this paper, we use the same scenario for the future urban expansion of Paris urban area until the end of the 21st century. It determines the size, shape and structure of the future city. Many other scenarios could have been used, in terms of spatial extent, shape, or urban design of new neighbourhoods. Some retroactions on local climate may occur. As an example, Adachi et al. (2014) and Lemonsu et al. (2015) have recently shown that the degree of urban compactness can impact the city vulnerability to heat-waves and the exposure of population to heat. Through the thermoregulation capacity of vegetation, the more greened the city is, the better the thermal comfort is.

To test this, we have simulated the consequences of the combined watering scenario (*C*) in an alternate urban expansion scenario. We have used a scenario in which it is supposed that policies have uniformly created new green spaces in the city. More precisely, we have used a scenario (created by NEDUM-2D model, cf. Section 3.1.2) in which we suppose that, in 2100, 10% of the urbanized surface of each point of our simulation grid has been converted into a park (it is one of the scenarios used in Lemonsu et al. (2015), see this article for more information on this scenario). The coverage of green spaces is increased in this case by 23%, and the city is more spread out. Because of this increased vegetation surface, we simulate that vegetation watering goes up

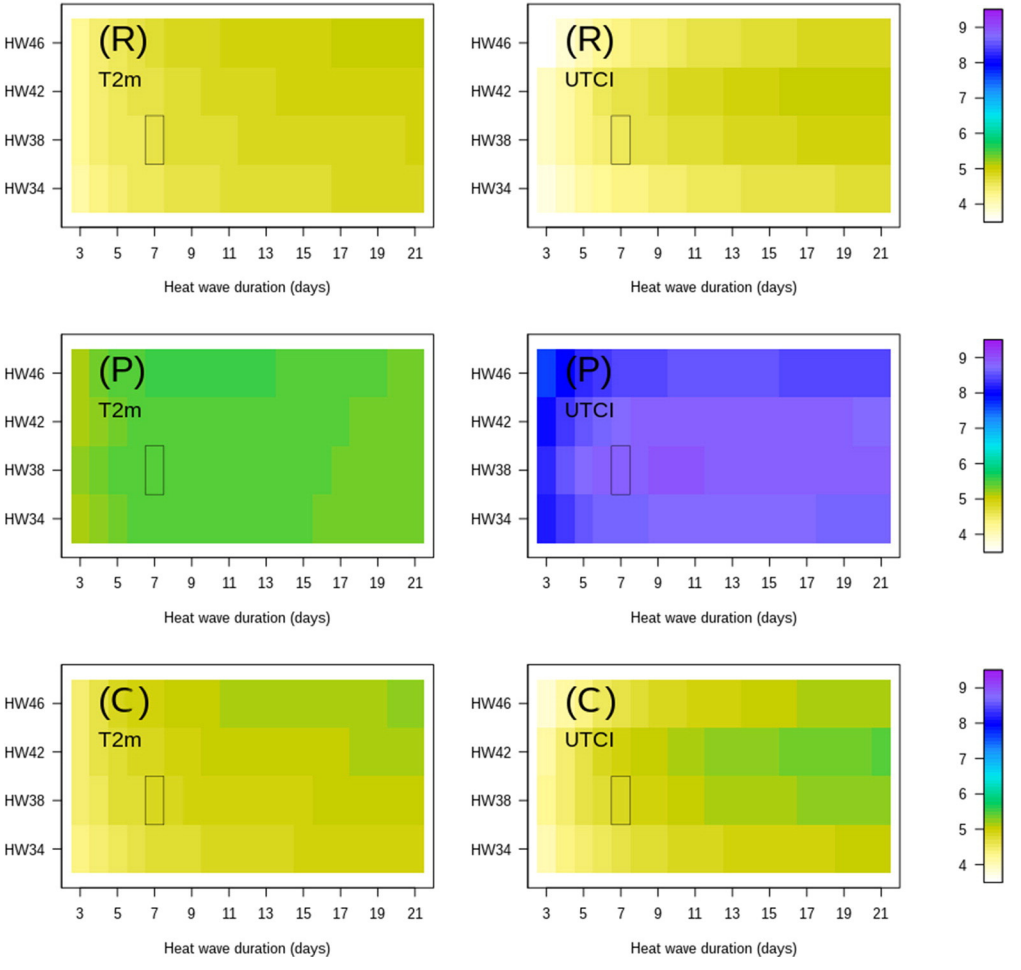

Fig. 7. Comparison of cooling efficiency of the different watering scenarios. The coefficient Eff is calculated based on 2-m air temperature (left) and UTCI (right), and is spatially aggregated over the city according to the map of urbanization rate. The black square indicates the cooling efficiency in the case of HW38 after seven days of heat wave.

to 6.03 Mm^3 of water per day. Despite this greater water consumption, the benefits in terms of mitigation of air temperature and heat stress are such that the coefficient of cooling efficiency is higher: 5.04 instead 4.66, and 4.89 instead 4.55, for $Eff_{(R)}$ and $EFF'_{(R)}$ respectively.

7.2. Heat-wave conditions

In this article, the analysis of processes and of impacts has been focused on specific heat wave conditions comparable to the 2003 heat wave, i.e. a heat wave of seven days with a daytime maximum temperature of 38 °C. In order to assess the sensitivity of scenarios and watering practices to the intensity and duration of heat waves, the coefficient of cooling efficiency has also been calculated for different heatwave lengths (from three days to three weeks) and for different heatwave intensities (cf. Section 3.1.1), namely HW34, HW38, HW42, and HW46 (see Fig. 7). One can note that these heatwave lengths and durations come from a statistical study over an ensemble of climate projections and are supposed to be representative of the future heatwaves in 2100. More details can be found in Lemonsu et al. (2014).

It is observed that efficiency of vegetation watering scenario (R) based on T2 m is increasing both with duration and intensity of heat waves. It is improved by about 15–19% between the beginning and the end of the three-week heat wave depending on the intensity. The efficiency is slightly better for the more intense heat waves.

The increase in cooling efficiency with the heat-wave length is still more noticeable when the coefficient is computed with UTCI. $Eff'_{(R)}$ increases by 12% for HW34 and by 36% for HW46 between the beginning and end of heat wave. However, when comparing the efficiencies $Eff'_{(R)}$ calculated for the different heat-wave intensities but for a same duration, it is shown that the efficiency is the best for HW38 and HW42. This means that the performances of vegetation watering in mitigating heat stress tend to slightly decline for very severe heat waves. For pavement watering, the cooling efficiency varies little in response to intensity and duration of heat waves. The highest values are reached for intermediate events, i.e. HW38 and HW42 with durations between one and two weeks. This is likely due to an irrigation rate more efficient for these intensities. For HW34, the cooling effect is lower and the water supply being the same, the efficiency coefficient is therefore lower. For HW46, there is likely not enough water supply to enhance a cooling effect as important as HW38 and HW42. Plants are quickly in water stress and evaporation occurs really fast on the roads, diminishing the impacts on air and radiant temperatures. In this case, however, the watering rate could be adapted to optimize evaporation, and alternate pavement watering schemes and rates might be more efficient than the one we simulate here. Finally, the combination of both watering practices in scenario (C) leads for a given intensity to a cooling efficiency which increases with heat-wave duration. As with (R), it is maximum for HW46 and HW42, when it is computed from T2 m. As explained above, when computed from UTCI, for a given duration, the highest efficiencies are obtained for HW38 and HW42.

7.3. Vegetation type

Finally, in our results, the types of vegetation layouts and of vegetation species play, a priori, an important role. We could not, however, assess properly the consequences of a change in these hypotheses. This issue would require the use of more sophisticated physiological models.

This is left for future work, as some important improvements are currently implemented in the TEB-ISBA model, and could enable to move forward on these issues. First, a new parameterization for radiative exchanges inside the canyon with the presence of street trees is underway in order to take into account the attenuation effects for ground-based surfaces and buildings due to the foliage. In addition, a more sophisticated parameterization of hydrological processes will be available soon. The objective is to better represent the water exchanges between atmosphere, surface and subsoil, especially the surface water runoff and the groundwater drainage toward the water networks.

8. Conclusions

Greening the city can be a relevant a tool to mitigate UHI in case of heat-wave. However, this study highlights that in order to preserve the cooling potential of vegetation, it is critical to insure it a sufficient water supply. Indeed, different irrigation strategies have been tested in order to mitigate the urban heat island

and improve population thermal comfort over the projected city of Paris in 2100. Using a set of indicators such as UHI intensities, minimal nighttime temperature, cooling efficiencies and water demand, these scenarios were evaluated and compared to a reference non irrigated scenario. It appears that without watering, the soils are drying and the vegetation is in water-stress condition, so that its evapotranspiration capacity is too weak to contribute to UHI mitigation. This highlights the critical issue of water storage and management.

In the present study, the scenario for which vegetation is watered according to an a priori realistic protocol results in a significant cooling of air temperature near the ground between 0.5 and 1.5 °C, both during daytime and nighttime. Despite reasonable watering rates, the implementation of such greening policies at the city scale leads to a very large total water consumption, which might for instance be higher than Seine river low flow at the end of the century.

Considering the simulation results, the benefits of vegetation for regulating the urban microclimate are undeniable over a large part of the city. Only the most urbanized areas are not impacted due to the too low coverage of vegetation. By concentrating population, they are however high-stake vulnerable areas. The pavement watering can be an interesting solution in such environment. It enables in a very local but significant cooling effect during the day for the city center and inner suburbs. The large-scale evaluation indicates that this strategy makes sense only in areas where the proportion of ground-based impervious surfaces is sufficiently important. It has the advantage that it can be activated occasionally with an immediate effect, and that water supplies can be easily adapted to optimize the evaporation. The water consumption is consequently much less important than for vegetation watering.

As a conclusion, the two strategies of watering that have been tested have complementary roles. They do not involve in the same physical processes, and are consequently efficient in different urban configurations, so that they can be combined for a better efficiency.

The study presented here is focused on heat waves, and the adaptation strategies aiming at reducing the vulnerability of city and population in such extreme conditions. In future works, it will be however crucial to extend the analysis to longer time periods in order to evaluate in a more complete way the proposed adaptation strategies. It will be also an appropriate framework to investigate the water cycle in urban environment, as well as the issue of sustainable and sensitive management of water resource.

Acknowledgments

This study benefited from funding by the French Agency for Research (ANR) through the VURCA project (ANR-08-VULN-013). The authors are grateful to the large VURCA's community, especially Stéphane Hallegatte for initiating the project. They also thank Colette Marchadier and Jean-Luc Salagnac for the elaboration of the database of building characteristics, as well as Anne-Lise Beaulant and Grégoire Pigeon for their contribution to the design and implementation of the modeling platform. Finally, they thank Cécile De Munck and Eric Martin for sharing some of their data information.

Appendix A. Description of urban expansion scenario

Within the frameworks of the VURCA project (see VURCA final report), integrated city prospective scenarios have been built to translate a possible evolutions of the city at the end of the century. They combine four potential action levers: urban-planning policies to manage the future urban sprawl, adaptation measures for buildings, air-conditioning usage, and watering practices. Each of them consists in different alternatives or hypotheses. In this study, we use one of these scenarios, the “SPR” scenario, which was used as a reference scenario and represents an extrapolation of existing trends.

The urban sprawl is simulated by the NEDUM-2D socio-economic model, forced by macro-economic trends of energy costs especially for oil and demographic pressure (Viguié et al., 2014). NEDUM-2D is a dynamic model which relies on the classical urban economics framework, an economic modeling approach developed in the end of the 1960s (Alonso, 1964; Mills, 1967; Muth, 1969) which explains the spatial distribution — across the city — of the costs of land and of real estate, housing surface, population density and buildings heights and density. It is based on three main mechanisms.

First, we suppose that households choose their accommodation location and size by making a trade-off between the time and money they spend in transport (i.e. to commute to their jobs) and the real estate price level (or, equivalently, between the proximity to the city center and the housing surface they can afford).

Second, real estate developers choose to build more or less housing (i.e. larger or smaller building) at a specific location, depending on the local level of real estate prices. When these prices are low, developers tend to build low density buildings, and when these prices are high, they tend to build high density buildings. Third, we suppose that various city characteristics do not evolve and adjust at the same speed. For instance, rents can evolve very quickly, whereas buildings change with a much longer timescale. Building depreciation is also very low, leading to path dependency and lockins in city evolution. Using these mechanisms, it is possible to determine the structure of the city from information on population size, households' income, transport network location, building construction costs and developers behavior parameters.

The reference scenario (*SPR*) corresponds to the scenario called "SN with high demographic hypothesis" in Viguié et al. (2014). Fig. 8 shows for instance the demographic scenario used in our simulations.

Appendix B. Modeling of evaporation processes in ISBA and TEB models

B.1. Modeling of evaporation and transpiration of natural covers in ISBA model

The ISBA model is able to simulate the physical processes related to physiological functioning of plants, and to soil water status evolution.

The soil moisture is governed for the soil layer (w_g, w_2 and w_3) by the following equations:

$$\frac{\partial w_g}{\partial t} = \frac{C_1}{\rho_w d_1}\left(I - E_g\right) - D_1 \tag{6}$$

$$\frac{\partial w_2}{\partial t} = \frac{1}{\rho_w d_2}\left(I - E_g - E_v\right) - K_2 - D_2 \tag{7}$$

$$\frac{\partial w_2}{\partial t} = \frac{d_2}{(d_3 - d_2)}(K_2 + D_2) - K_3 \tag{8}$$

where K_* and D_* represent respectively the gravitational drainage of soil water and the vertical soil moisture diffusion. d_1, d_2, d_3 are respectively the superficial soil depth, the rooting layer depth and the total modeled soil depth. C_1 is a dimensionless surface restore coefficient and ρ_w is the water density.

I represents the infiltration rate. E_g and E_v are the evaporation from the ground and of evapotranspiration from the vegetation.

ISBA represents the surface as a combination of vegetation (with a cover fraction referred to as f_{veg}) and of bare soil (1-f_{veg}) and uses a composite surface temperature (T_s) to compute these surface exchanges:

$$E_g = \left(1 - f_{veg}\right)\rho_a C_h V_a (h_u q_{sat}(T_s) - q_a) \tag{9}$$

$$E_v = f_{veg}\rho_a C_h V_a (h_v q_{sat}(T_s) - q_a) \tag{10}$$

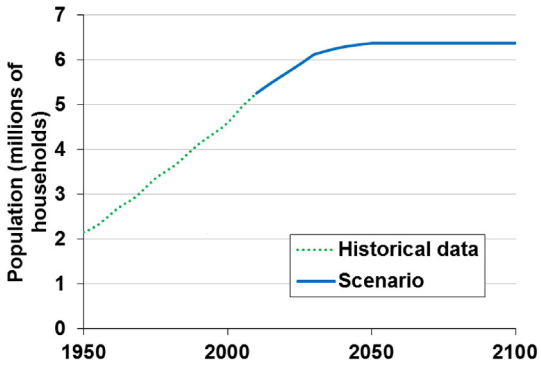

Fig. 8. Demographic scenario used in the simulations.

The atmospheric conditions are defined by ρ_a, V_a and q_a are respectively the air density (ρ_a), the wind speed (V_a), and the atmospheric specific humidity (q_a) Surface conditions are determined using the saturated specific humidity at surface level ($q_{sat}(T_s)$), the relative humidity at the ground surface (h_u), and the Halstead coefficient (h_v) which accounts for direct evaporation from the fraction of the foliage covered by intercepted water and for transpiration of the remaining part of the leaves. This coefficient depends on radiation, water stress, atmospheric vapor pressure and air temperature through a Jarvis resistance. Finally, the exchanges are driven by a drag coefficient (C_h) which depends on the thermal stability of atmosphere. Evaluation were first performed by Noilhan and Planton (1989) and then by Boone et al. (1999) for the inclusion of the subroot layer in ISBA model.

B.2. Modeling of evaporation over impervious covers in TEB model

The TEB models deals with water exchanges between impervious surfaces and atmosphere. It represents rainwater interception on roads and roofs, evaporation of available water, and surface runoff.

A water reservoir is attributed to each of them, for which the water content is calculated and updated at each model time step. The reservoir fills with rainfall, and it empties itself through surface evaporation process. When water content exceeds the maximum interception capacity, the water excess is discharged by surface runoff toward sewer. For the roads, the maximum interception capacity W_{max} is prescribed to 1 mm of water. This default value is in accordance with the orders of magnitude found in the literature (Grimmond et al. (1991), Lemonsu et al. (2007)). The implementation of pavement watering in TEB is based on this parameterization, simply by treating this water supply the same way than rainfall.

Thus, pavement watering suppose an increase of the rainfall value R in the water-reservoir evolution equation in TEB:

$$\frac{\partial W}{\partial t} = R - \frac{LE}{L_v} \quad (W < W_{\max}) \tag{11}$$

where W is the water reservoir, LE the latent heat flux, and L_v the latent heat of vaporization.

References

Adachi, S.A., Kimura, F., Kusaka, H., Duda, M.G., Yamagata, Y., Seya, H., ... Aoyagi, T., 2014. Moderation of summertime heat island phenomena via modification of the urban form in the Tokyo metropolitan area. J. Appl. Meteorol. Climatol. 53 (8), 1886–1900.

Alexandri, E., Jones, P., 2008. Temperature decreases in an urban canyon due to green walls and green roofs in diverse climates. Build. Environ. 43 (4), 480–493.

Alonso, W., 1964. Location and Land Use. Toward A General Theory of Land Rent .

Basara, J.B., Basara, H.G., Illston, B.G., Crawford, K.C., 2010. The impact of the urban heat island during an intense heat-wave in Oklahoma City. Adv. Meteorol. 2010.

Beniston, M., 2004. The 2003 heat wave in Europe: a shape of things to come? An analysis based on Swiss climatological data and model simulations. Geophys. Res. Lett. 31 (2).

Boone, A., Calvet, J.C., Noilhan, J., 1999. Inclusion of a third soil layer in a land surface scheme using the force-restore method. J. Appl. Meteorol. 38 (11), 1611–1630.

Bowler, D.E., Buyung-Ali, L., Knight, T.M., Pullin, A.S., 2010. Urban greening to cool towns and cities: a systematic review of the empirical evidence. Landsc. Urban Plan. 97 (3), 147–155.

Bueno, B., Pigeon, G., Norford, L.K., Zibouche, K., Marchadier, C., 2012. Development and evaluation of a building energy model integrated in the TEB scheme. Geosci. Model Dev. 5, 433–448.

de Munck, C., 2013. Modélisation de la végétation urbaine et des stratégies d'adaptation au changement climatique pour l'amélioration du confort climatique et de la demande énergétique en ville. PhD Thesis. Paul Sabatier University, Toulouse, France in French.

de Munck, C., Pigeon, G., Masson, V., Meunier, F., Bousquet, P., Tréméac, B., ... Marchadier, C., 2013. How much can air conditioning increase air temperatures for a city like Paris, France? Int. J. Climatol. 33 (1), 210–227.

Déqué, M., Rowell, D.P., Lüthi, D., Giorgi, F., Christensen, F.H., Rockel, B., Jacob, D., Kjellström, E., de Castro, M., van den Hurk, B., 2007. An intercomparison of regional climate simulations for Europa: assessing uncertainties in model projections. Clim. Chang. 81, 53–70.

Ducharne, A., Gascoin, S., Habets, F., Ledoux, E., Martin, E., Oudin, L., ... Viennot, P., 2009. Projet RExHySS. Annexe Volet 2. Description des modèles hydrologiques in French.

Fiala, D., Havenith, G., Bröde, P., Kampmann, B., Jendritzky, G., 2012. UTCI-Fiala multi-node model of human heat transfer and temperature regulation. Int. J. Biometeorol. 56, 429–441.

Fujita, M., 1989. Urban Economic Theory: Land Use and City Size. Cambridge University Press book. (366pp).

Gabriel, K.M., Endlicher, W.R., 2011. Urban and rural mortality rates during heat-waves in Berlin and Brandenburg, Germany. Environ. Pollut. 159 (8), 2044–2050.

Gaffin, S.R., Rosenzweig, C., Kong, A.Y., 2012. Adapting to climate change through urban green infrastructure. Nat. Clim. Chang. 2 (10), 704.
Giorgi, F., 2006. Climate change hot-spots. Geophys. Res. Lett. 33. http://dx.doi.org/10.1029/2006GL025 734.
Grimmond, C.S.B., Cleugh, H.A., Oke, T.R., 1991. An objective urban heat storage model and its comparison with other schemes. Atmos. Environ. Part B. Urban Atmos. 25 (3), 311–326.
Hamdi, R., Masson, V., 2008. Inclusion of a drag approach in the town energy balance (TEB) scheme: offline 1-d validation in a street canyon. J. Appl. Meteorol. Climatol. 47, 2627–2644.
Hamin, E.M., Gurran, N., 2009. Urban form and climate change: balancing adaptation and mitigation in the US and Australia. Habitat Int. 33 (3), 238–245.
Hémon, D., Jougla, E., Clavel, J., Laurent, F., Bellec, S., Pavillon, G., 2003. Surmortalité liée à la canicule d'août 2003 en France. Bull. Epidémiol. Hebd. 45–46 in French.
Hendel, M., Colombert, M., Diab, Y., Royon, L., 2015. An analysis of pavement heat flux to optimize the water efficiency of a pavement-watering method. Appl. Therm. Eng. 78, 658–669.
IPCC, 2015. Working group II Report "Impacts, Adaptation and Vulnerability" contribution to AR5. Current and Future Trends (Chapter 23).
Jaffal, I., Ouldboukhitine, S.E., Belarbi, R., 2012. A comprehensive study of the impact of green roofs on building energy performance. Renew. Energy 43, 157–164.
Kolokotsa, D., Rovas, D., Kosmatopoulos, E., Kalaitzakis, K., 2011. A roadmap towards intelligent net zero-and positive-energy buildings. Sol. Energy 85 (12), 3067–3084.
Kounkou-Arnaud, R., Desplat, J., Lemonsu, A., Salagnac, J.L., 2014. Epicea: étude des impacts du changement climatique à Paris. Météorologie 84, 42–48 in French.
Laaidi, K., Zeghnoun, A., Dousset, B., Bretin, P., Vandentorren, S., Giraudet, E., Beaudeau, P., 2012. The impact of heat islands on mortality in Paris during the August 2003 heat wave. Environ. Health Perspect. 120 (2), 254.
Lafore, J.-P., Stein, J., Asencio, N., Bougeault, P., Ducrocq, V., Duron, J., Fischer, C., Hreil, P., Mascart, P., Masson, V., Pinty, J., Redelsperger, J.L., Richard, E., de Arellano, J.V.G., 1998. The Meso-NH atmospheric simulation system. Part I: adiabatic formulation and control simulation. Ann. Geophys. 16:90–109. http://dx.doi.org/10.1007/s00585-997-0090-6.
Lambert-Habib, M.L., Hidalgo, J., Fedele, C., Lemonsu, A., Bernard, C., 2013. How is climatic adaptation taken into account by legal tools? Introduction of water and vegetation by French town planning documents. Urban Climate 4, 16–34.
Lemonsu, A., Masson, V., Berthier, E., 2007. Improvement of the hydrological component of an urban soil–vegetation–atmosphere–transfer model. Hydrol. Process. 21 (16), 2100–2111.
Lemonsu, A., Masson, V., Shashua-Bar, L., Erell, E., Pearlmutter, D., 2012. Inclusion of vegetation in the town energy balance model for modelling urban green areas. Geosci. Model Dev. 5 (6), 1377–1393.
Lemonsu, A., Kounkou-Arnaud, R., Desplat, J., Salagnac, J.L., Masson, V., 2013. Evolution of the Parisian urban climate under a global changing climate. Clim. Chang. 116 (3–4), 679–692.
Lemonsu, A., Beaulant, A.L., Somot, S., Masson, V., 2014. Evolution of occurrences of heat-waves over the Paris basin (France) in the 21st century. Clim. Res. http://dx.doi.org/10.3354/cr01235 .
Lemonsu, A., Viguié, V., Daniel, M., Masson, V., 2015. Vulnerability to heat-waves: impact of urban expansion scenarios on urban heat island and heat stress in Paris (France). Urban Climate 14, 586–605.
Li, D., Bou-Zeid, E., 2013. Synergistic interactions between urban Heat Islands and heat-waves: the impact in cities is larger than the sum of its parts. J. Appl. Meteorol. Climatol. 52 (9), 2051–2064.
Malys, L., Musy, M., Inard, C., 2014. A hydrothermal model to assess the impact of green walls on urban microclimate and building energy consumption. Build. Environ. 73, 187–197.
Marchadier, C., Pigeon, G., Salagnac, J.-L., 2012. Les scénarios«bâti et usages de la climatisation»et leur simulation (Developing and modeling of scenarios for buildings and air-conditioning usage). Technical Note. VURCA research project in French. (available online: http://www.cnrm.meteo.fr/ville.climat/spip.php?action=acceder_document&arg=447&cle=172af20584ccff3f8c8a9ae58c804dde957d6e48&file=pdf%2Fmethodo_scen_bati_v2.0.pdf).
Masson, V., 2000. A physically-based scheme for the urban energy budget in atmospheric models. Bound.-Layer Meteorol. 94, 357–397.
Masson, V., Lion, Y., Peter, A., Pigeon, G., Buyck, J., Brun, E., 2013b. Grand Paris: regional landscape change to adapt city to climate warming. Clim. Chang. 117 (4):769–782. http://dx.doi.org/10.1007/s10584-012-0579-1.
Middel, A., Brazel, A.J., Gober, P., Myint, S.W., Chang, H., Duh, J.D., 2012. Land cover, climate, and the summer surface energy balance in Phoenix, AZ, and Portland, OR. Int. J. Climatol. 32 (13), 2020–2032.
Mills, E.S., 1967. An aggregative model of resource allocation in a metropolitan area. Am. Econ. Rev. 197–210.
Muth, R.F., 1969. Cities and housing. The Spatial Pattern of Urban Residential Land Use. University of Chicago .
Noilhan, J., Planton, S., 1989. A simple parameterization of land surface processes for meteorological models. Mon. Weather Rev. 117, 536–549.
Pigeon, G., Zibouche, K., Bueno, B., Le Bras, J., Masson, V., 2014. Improving the capabilities of the town energy balance model with up-to-date building energy simulation algorithms: an application to a set of representative buildings in Paris. Energ. Buildings 76, 1–14.
Potchter, O., Cohen, P., Bitan, A., 2006. Climatic behavior of various urban parks during hot and humid summer in the Mediterranean city of Tel Aviv, Israel. Int. J. Climatol. 26 (12), 1695–1711.
Rosenzweig, C., Solecki, W.D., Hammer, S.A., Mehrotra, S. (Eds.), 2011. Climate Change and Cities: First Assessment Report of the Urban Climate Change Research Network. Cambridge University Press book.
Santamouris, M., Kolokotsa, D., 2013. Passive cooling dissipation techniques for buildings and other structures: the state of the art. Energ. Buildings 57, 74–94.
Shashua-Bar, L., Hoffman, M.E., 2000. Vegetation as a climatic component in the design of an urban street: an empirical model for predicting the cooling effect of urban green areas with trees. Energ. Buildings 31 (3), 221–235.
Shashua-Bar, L., Pearlmutter, D., Erell, E., 2011. The influence of trees and grass on outdoor thermal comfort in a hot-arid environment. Int. J. Climatol. 31 (10), 1498–1506.
Solecki, W.D., Rosenzweig, C., Parshall, L., Pope, G., Clark, M., Cox, J., Wiencke, M., 2005. Mitigation of the heat island effect in urban New Jersey. Global Environ. Change B. Environ. Hazard 6 (1), 39–49.

Souch, C.A., Souch, C., 1993. The effect of trees on summertime below canopy urban climates. J. Arboric. 19, 303.
Stone Jr., B., Rodgers, M.O., 2001. Urban form and thermal efficiency: how the design of cities influences the urban heat island effect. J. Am. Plan. Assoc. 67 (2), 186–198.
Takahashi, R., Asakura, A., Koike, K., Himeno, S., Fujita, S., 2010. Using snow melting pipes to verify water sprinkling's effect over a wide area. Sustainable Techniques and Strategies in Urban Water Management 2010. NOVATECH, p. 10.
Tan, J., Zheng, Y., Tang, X., Guo, C., Li, L., Song, G., ... Chen, H., 2010. The urban heat island and its impact on heat-waves and human health in Shanghai. Int. J. Biometeorol. 54 (1), 75–84.
Vautard, R., Beekmann, M., Desplat, J., Hodzic, A., Morel, S., 2007. Air quality in Europe during the summer of 2003 as a prototype of air quality in a warmer climate. Compt. Rendus Geosci. 339 (11), 747–763.
Viguié, V., Hallegatte, S., Rozenberg, J., 2014. Downscaling long term socio-economic scenarios at city scale: a case study on Paris. Technol. Forecast. Soc. Chang. 87, 305–324.
Wark, C.G., Wark, W.W., 2003. Green roof specification & standards. Connect. Specif. 56 (8), 76–82.